Cosecant-Squared Radiation Pattern Synthesis of Conformal Microstrip Arrays

Sidi Ahmed Djennas, Fethi Tarik Bendimerad

Laboratory of Telecommunications,
Faculty of Science Engineering, Abou-Bekr Belkaïd University – Tlemcen,
P. O. Box 230, 13000 Tlemcen, Algeria.

***Abstract*— Contrary to the rectilinear and planar arrays, the conformal arrays are very suitable for enlightening the hidden zones. In this paper we will carry out the cosecant-squared radiation pattern synthesis of conformal microstrip arrays. This aim will be achieved by the use of a deterministic optimization method that developed for this type of arrays. This synthesis and by means of the results which that procure, constitutes a database for the radar applications, targets tracking, satellites and radio guidance.**

***Key words*— Conformal array, synthesis, optimization.**

I. INTRODUCTION

THE Omni-directional illumination of space imposes the electromagnetic coverage of the whole observation sphere, including the hidden zones.

Unfortunately, this particularity remains impossible for the planar and rectilinear arrays where the illuminated zone is limited to the higher half space upon the array carrier plane [1]–[4].

The solution would be thus to bend the carrier surface for extending the radiation to the lower half space.

By applying a feeding law to the array, we can diversify the shapes of the radiation pattern. It is by exploiting this key parameter that we will synthesize the radiation pattern specifically to a desired function [1], [2], [5].

In this paper, the desired pattern that we label the cosecant-squared pattern (CSP) and where the main area will take an oblique appearance, has a more complex and different form compared with the conventional window pattern [1], [2], [6], [7].

The synthesis process aims the minimization of the deviation between the computed pattern and the CSP. This operation requires optimization techniques such as the variational method which was specifically developed for the conformal arrays [1], [2].

These arrays, takes more importance in studies and researches for the civilian and military communication systems, because they can be implanted on all bent surfaces : aircraft fuselage, airfoil, missile nose, radar radome, etc.

II. CONFORMATION RESTRICTIONS

The differences between conformal and planar arrays, are the distribution of the elements and the elementary pattern.

For the planar arrays, the equidistant spacing between elements allows a simplified writing of the far-field pattern formula [7]. Moreover, the look angle of the elements are the same as it is shown on Fig. 1.

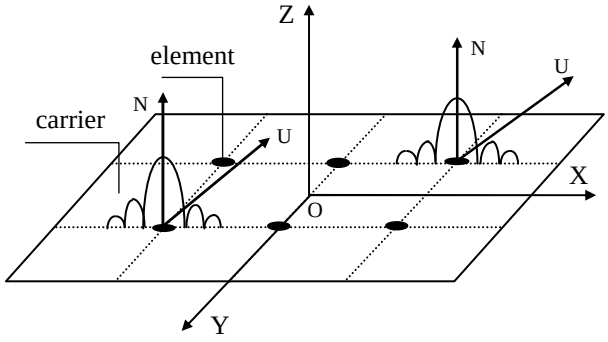

Fig. 1. Elementary pattern, planar case

For the conformal array, the look unit vectors are non-equipollents. Consequently the element pattern must been determined by measurement or computation.

Indeed, all elements are not seen by the same direction, this is very clear on Fig. 2.

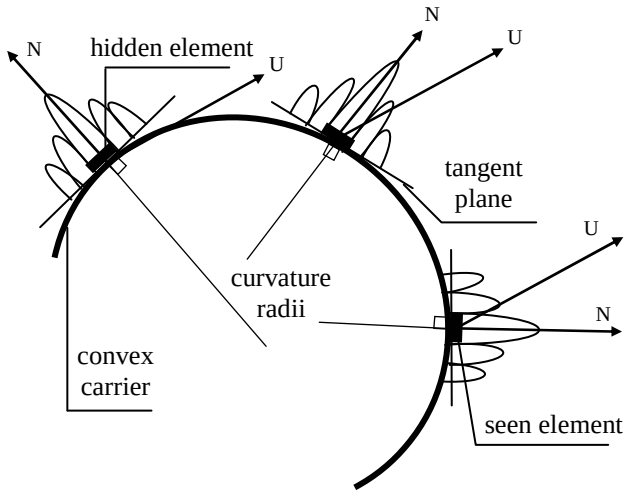

Fig. 2. Elementary pattern, conformal case

A simple test on the scalar product of the propagation vector and the normal vector depicted on Fig. 3, reveals us if the element is seen or hidden. This normal represents the main radiation direction. It is defined as being the perpendicular to the tangent plane on the element surface.

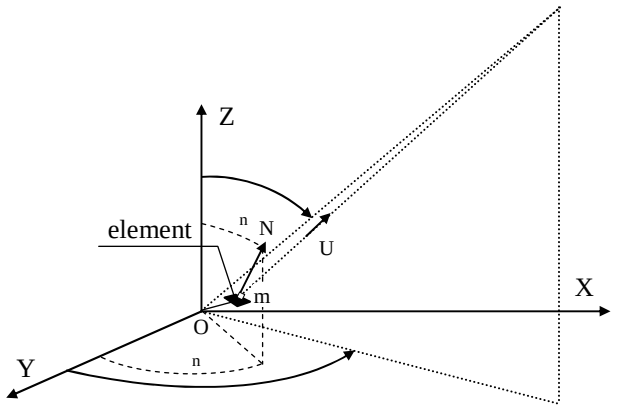

Fig. 3. Associated vectors to the visibility test global coordinates system

The necessary condition for seen element is :

$$\vec{U} \,.\, \vec{N} \geq 0 \qquad (1)$$

$\vec{U}$: propagation direction vector,

$\vec{N}$: normal vector, defined by angles θ_n , φ_n .

The conformal structure call for the transformation of coordinates systems. This operation is carried out by two rotations. The first one, runs around the Z-axis, with φ_n , the second one, runs around the new Y-axis, with θ_n , giving rise to the n^{th} element local coordinates system.

In order to determine exactly the far-field values in the global coordinates system, being known those of the local coordinates system, we build a transformation matrix given by formula (2).

$$MP = \begin{bmatrix} \cos\theta_n \cos\varphi_n & \cos\theta_n \sin\varphi_n & -\sin\theta_n \\ -\sin\varphi_n & \cos\varphi_n & 0 \\ \sin\theta_n \cos\varphi_n & \sin\theta_n \sin\varphi_n & \cos\theta_n \end{bmatrix} \qquad (2)$$

Thus, The algebraic expression of the propagation vector in the local coordinates system becomes :

$$\vec{U}' = MP \,.\, \vec{U} \qquad (3)$$

This expression will make it possible to define for any direction, the far-field values.

III. PROBLEM AND SOLUTION STATEMENTS

The far-field pattern for a N_s -elements array is given by the expression :

$$f(\theta,\varphi) = \sum_{n\ 1}^{n\ N_s} a_n \, e^{\,j\frac{2\pi}{\lambda}(om_n\ u)} \, E_n(\theta,\varphi) \qquad (4)$$

With :

$f(\theta,\varphi)$: far-field pattern magnitude,

a_n : n^{th} element complex feed,

λ : wavelength,

$\vec{om}_n$: n^{th} element position vector defined in the global coordinates system,

$E_n(\theta,\varphi)$: n^{th} elementary pattern,

θ , φ : are respectively the elevation and azimuth angular coordinates of the observation point.

The starting point for our problem is the far-field pattern specified by the CSP. The array feeding law is the unknown factor to be determined [1], [2], [7]. The ultimate condition for optimal solution is given by the formula :

$$M_l(\theta,\varphi) \leq f(\theta,\varphi) \leq M_u(\theta,\varphi) \qquad (5)$$

Where :

M_u : upper level of the CSP,

M_l : lower level of the CSP.

We will choose as for any optimization method a functional J which we write in the following form :

$$J = \iint_{D1} L(\theta,\varphi)\, p(\theta,\varphi) d\theta\, d\varphi + \iint_{D2} \left| f(\theta,\varphi) \right|^2 d\theta\, d\varphi \qquad (6)$$

With :

$L(\theta,\varphi)$: function evaluating the variation between the synthesized pattern and the desired pattern (CSP),

$p(\theta,\varphi)$: weighting function,

D1, D2 : are by order, the useful and useless coverage region.

In first, we set a variation of J. Next, by expressing the nullity of this variation, we obtain a nonlinear equations system of N_s unknown factors formulated by the expression (7).

$$\sum_{m\ 1}^{m\ N_s} a_m \iint_{D1\ D2} e^{\,j\frac{2\pi}{\lambda}(om_m\ \ om_n)u} \, E_m \, E_n \, d\theta\, d\varphi = \iint_{D1} \left[\left(\frac{M_u + M_l}{2f} - 1 \right) p + 1 \right] f \, e^{\,j\frac{2\pi}{\lambda}(om_n u)} \, E_n \, d\theta\, d\varphi \qquad (7)$$

We can rewrite the expression (7) in compact matrix form, so we obtain :

$$\sum_{m\ 1}^{m\ N_s} a_m \, I_{m,n} = b_n \qquad (8)$$

As Fig. 4 show it, the numerical solving of this system will be achieved by successive iterations, starting from an arbitrary feed law.

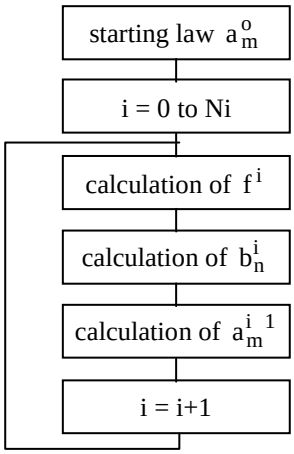

Fig. 4. Flowchart of numerical solving

IV. CSP SETTING

The desired pattern is defined by various parameters. These parameters appear on Fig. 5 for a revolution view and on Fig. 6 for a projected view.

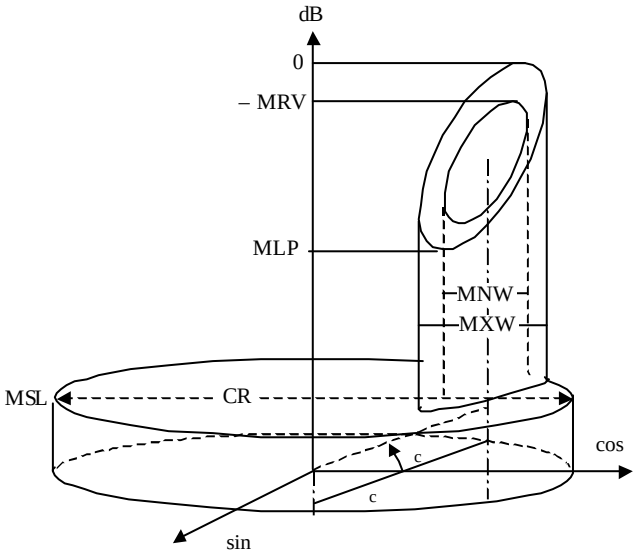

Fig. 5. CSP in revolution view

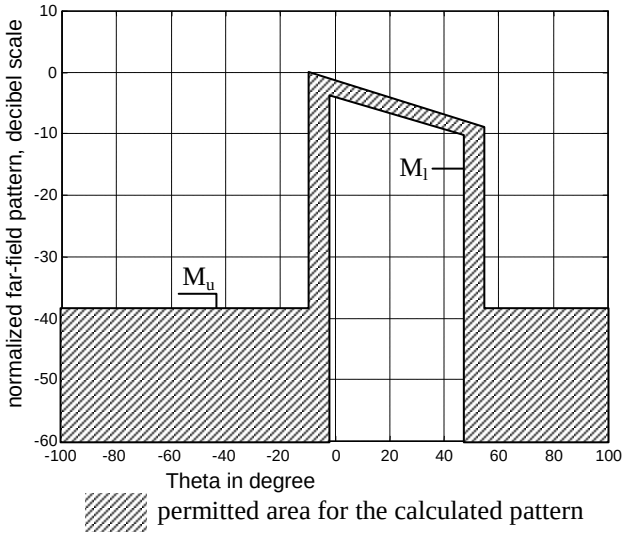

Fig. 6. CSP in projected view, φ_c plane

The parameters that defines the CSP are :
The main-lobe major peak fixed at 0 dB,
The main-lobe minor peak in decibels : MLP,
The maximum ripple value in decibels : MRV,
The maximum sidelobe level in decibels : MSL,
The major beamwidth in degrees : MXW,
The minor beamwidth in degrees : MNW,
The elevation and azimuth scan angles in degrees : θ_c and φ_c ,
The useful coverage region in degrees : UCR.

V. RESULTS AND COMMENTS

A.. Rooftop array

As it is shown on Fig. 7, the rooftop array is composed of two inclined planes. The eight elements operates at the frequency of 5 GHz. The inter-element spacing is of $0.5\,\lambda$.

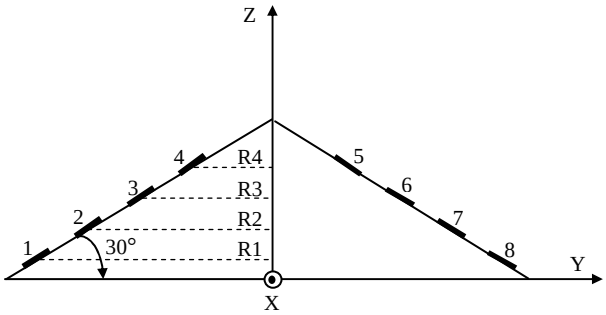

Fig. 7. Rooftop array

R1 = 9.09 cm, R2 = 6.49 cm, R3 = 3.89 cm, R4 =1.29 cm.

- CSP parameters

For the rooftop array, the CSP is restricted by the following parameters :
MLP = – 5 dB, MRV = 3 dB, MSL = – 30 dB, MXW = 70° , MNW = 40° , UCR = 360° .

The synthesis results for a shifted CSP are plotted on Fig. 8 and Fig. 10 for all space and on Fig. 9 and Fig. 11 for plane cuts.

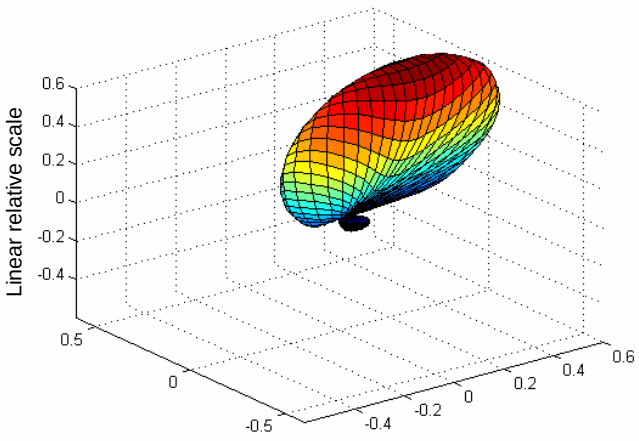

Fig 8. 3-D radiation pattern plot, rooftop array

$\theta_c = -30^\circ$, $\varphi_c = 45^\circ$

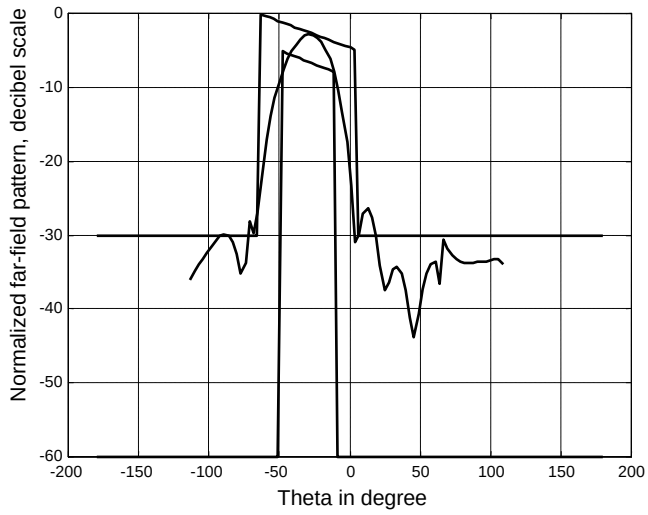

Fig. 9. CSP and synthesized pattern, rooftop array plane cut $\varphi_c = 45$

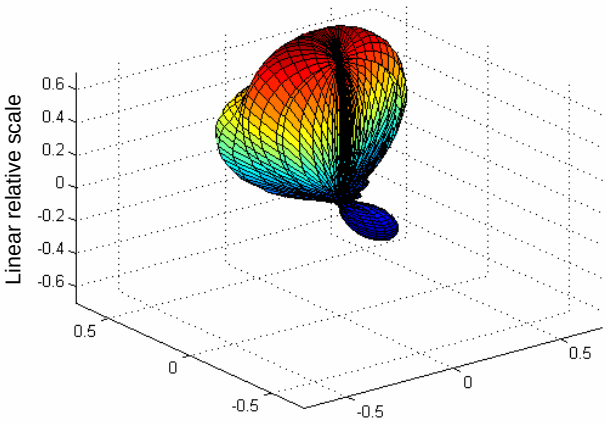

Fig. 10. 3-D radiation pattern plot, rooftop array $\theta_c = 20$, $\varphi_c = 60$

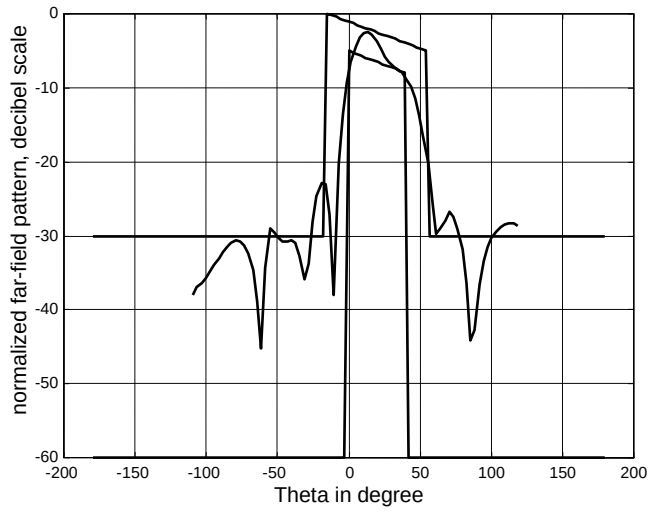

Fig. 11. CSP and synthesized pattern, rooftop array plane cut $\varphi_c = 60$

B. Cone array

The second array which is depicted on Fig. 12 is cone-shaped one. The working frequency is of 3 GHz. This array is composed of 82 elements distributed on 6 rings. The inter-ring spacing is of $0.8\,\lambda$.

The top, bottom rings have the radii of 5.09 cm, 22.39 cm. The inter-element spacing on rings varies from $0.6\,\lambda$ to $0.8\,\lambda$.

The numbers of elements by ring and on the vertex-base direction are : 22, 20, 16, 12, 8, 4.

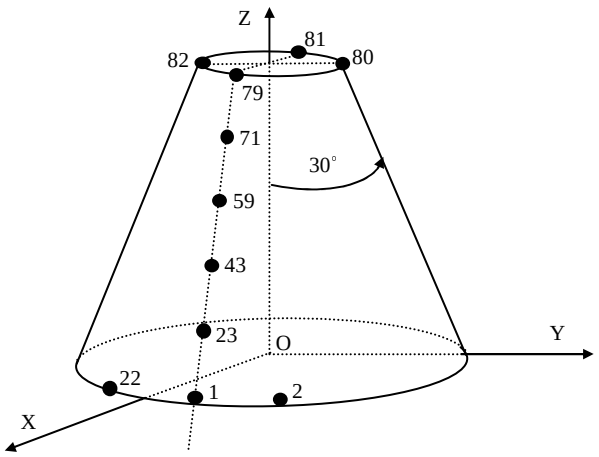

Fig. 12. Cone array

- CSP setting

For this second array, the CSP is defined by the following parameters :
MLP = – 10 dB, MRV = 2 dB, MSL = – 30 dB, MXW = 60° , MNW = 40° , UCR = 180° .

In the case of a broadside CSP the obtained results are sketched on Fig. 13 for all space and on Fig. 14 for plane cut. Fig. 15 and Fig. 16 are plotted for the shifted CSP case.

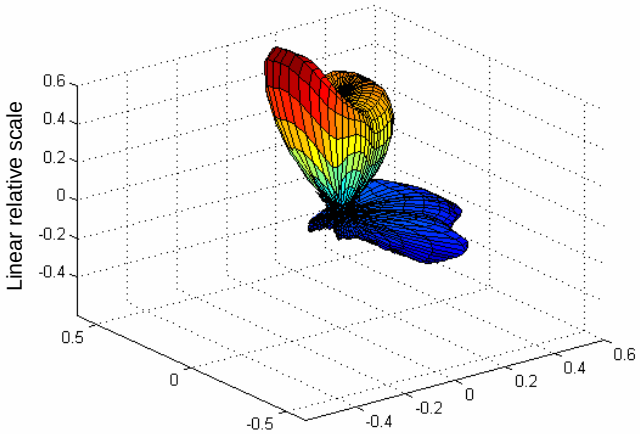

Fig. 13. 3-D radiation pattern plot, cone array $\theta_c = 0^\circ$, $\varphi_c = 0^\circ$

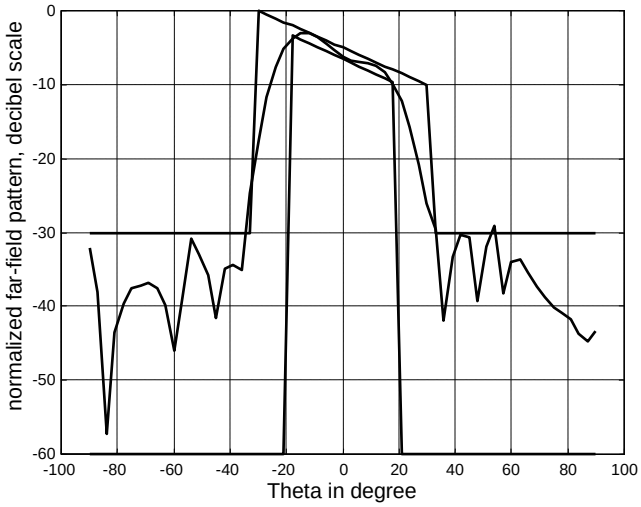

Fig. 14. CSP and synthesized pattern, cone array plane cut, $\varphi_c = 0$

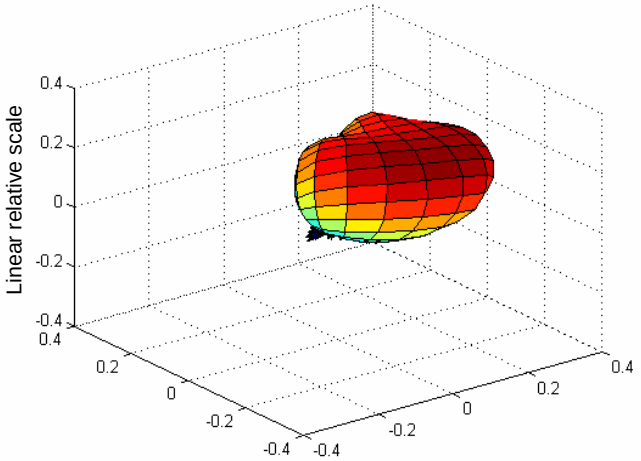

Fig. 15. 3-D radiation pattern plot, cone array $\theta_c = -45$, $\varphi_c = 60$

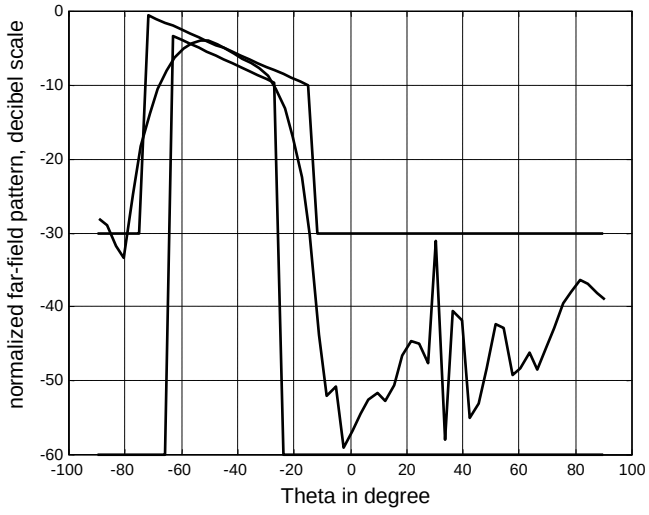

Fig. 16. CSP and synthesized pattern, cone array plane cut $\varphi_c = 60$

Generally speaking, we can qualify our findings through the graphical results as very satisfactory since the CSP restrictions are well respected.

VI. Conclusion

In this paper we have discuss the conformal microstrip arrays synthesis.

The setting up of these arrays upon the convex bodies allows in addition to the targets localization, to widen the scanning domain and so to enlighten even the hidden zones, from where the importance of such structures.

The studied cases, from the simplest one which is the rooftop array, to the most complex which is the cone array, generates very satisfactory results, even if a variation always separates the desired pattern from the computed one.

References

[1] S. A. Djennas, F. T. Bendimerad, ‘‘ Synthèse du Rayonnement d’Antennes Imprimées Disposées en Réseaux Conformes Convexes ’’, *Conférence sur le Génie Electrique, CGE’01*, December 2001, pp. 27.

[2] Sidi Ahmed Djennas, Fethi Tarik Bendimerad, ‘‘ Electromagnetic Beam Synthesis of Micro-Strip Antennas Implanted on Bent Carrier Bodies ’’, *First Algerian Conference on Microelectronics, ACM’ 02*, October 2002, pp. 348–352.

[3] J. P. Damiano, M. Scotto, J. M. Ribero, ‘‘ New Application of an Application Tool to Fast Analysis and Synthesis of Conformal Printed Antenna ’’, *Electronic Letters*, vol. 32, no. 22, September 1996, pp. 2033-2035.

[4] T. Girard, R. Staraj, E. Cambiaggio, F. Muller, ‘‘ Synthesis on Conformal Antenna Array ’’, *Millennium Conference on Antennas & Propagation, A.P. 2000*, April 2000.

[5] Y. U. Kim and J. D. Nespor, ‘‘ Shaped Beam Synthesis and Conditional Thinning for Planar Phased Array ’’, *IEEE/AP-S Int. Symp. URSI Radio Sci. Meet*, vol. 2, July 1996, pp. 802–805.

[6] J. A. Rodriguez, E. Botha, F. Ares, ‘‘ Extension of the Orchard–Elliott Synthesis Method to Pure-Real Nonsymmetrical-Shaped Patterns ’’, *IEEE. Transactions on Antennas and Propagation*, vol. 45, no. 8, August 1997, pp. 1317–1319.

[7] O. M. Bucci, G. D'Elia, G. Romito, ‘‘ Power Synthesis of Conformal Arrays by a Generalized Projection Method ’’, *IEE Proc.- Microw. Antennas Propag.* vol. 142, no. 6, December 1995, pp. 467-471.